Int J Clin Exp Med 2016;9(3):5574-5583
www.ijcem.com /ISSN:1940-5901/IJCEM0018272

Original Article

Genome-wide differential gene expression profiling of bone marrow cells in diabetes mellitus type 2 mice

Junjie Yang[1*], Wenying Yan[2*], Chuanlu Ren[3], Xizhe Li[4], You Zhang[5], Takayuki Asahara[6], Zhenya Shen[1]

[1]Department of Cardiovascular Surgery of The First Affiliated Hospital, Institute for Cardiovascular Science, Soochow University, Suzhou, China; [2]Center for Systems Biology, Soochow University, Suzhou, China; [3]Department of Clinical Laboratory, The 100th Hospital of PLA, Suzhou, China; [4]Department of Cardiovascular Surgery, Affiliated Shanghai 1st People's Hospital, Shanghai Jiaotong University, Shanghai, China; [5]Department of Cardiology, The First Affiliated Hospital of Soochow University, Suzhou, China; [6]Department of Regenerative Medicine, Tokai University School of Medicine, Kanagawa, Japan. [*]Equal contributors.

Received October 21, 2015; Accepted November 5, 2015; Epub March 15, 2016; Published March 30, 2016

Abstract: Aims: More and more studies pointed out that bone marrow was the primary target of diabetes mellitus-induced damage. The aim of this study was to determine whether the bone marrow cells in diabetes mellitus type 2 mice exhibit distinct gene expression profiles compared with normal ones. Methods: We performed global gene expression analysis in the bone marrow cells of diabetic mice and non-diabetic mice using Affymetrix Gene Chip Mouse Gene 1.0 ST Arrays. The gene expression patterns of diabetic mice were compared with those of nondiabetic ones using bioinformatics analysis. Validation of microarray results was examined by quantitative RT-PCR. Results: We identified 95 differentially expressed genes in diabetic mice (> or = 1.5 fold and p value < 0.05). Of these, 74 were down-regulated and 21 were up-regulated in the diabetic mice. Downregulated genes in diabetic bone marrow included chemotaxic genes, interferon inducible genes and genes involved in signal transduction. Upregulated genes in diabetic bone marrow included genes related to angiogenesis and genes associated with cardioprotection. Differentially expressed genes were further analyzed to find out the related biological processes and pathways. Pathways regulated in the db/db bone marrow include RIG-I-like receptor signaling pathway, chemokine signaling pathway, Toll-like receptor signaling pathway and cytosolic DNA-sensing pathway. Conclusions: Our investigation provides comprehensive gene information associated with impaired angiogenesis and migration of bone marrow cells in diabetic mice and the development of diabetes mellitus. This type of molecular profiling may facilitate future studies on molecular mechanisms governing core properties of these cells.

Keywords: Diabetes mellitus, bone marrow cells, microarray

Introduction

Diabetes is a group of metabolic diseases characterized by hyperglycemia resulting from defects in insulin secretion, insulin action, or both. The chronic hyperglycemia of diabetes is associated with long-term damage, dysfunction, and failure of different organs, especially the eyes, kidneys, nerves, heart, and blood vessels. Substantial clinical and experimental evidence suggests that endothelial dysfunction is a crucial early step in the development of diabetes, which is characterized by impaired endothelium-dependent vasodilation and endothelial activation [1]. However, following the discovery of endothelial progenitor cells (EPCs), researchers have attributed the defective re-endothelisation and neoangiogenesis in diabetes to that EPCs were reduced in numbers and impaired in the regenerative capacity in diabetes [2, 3]. The reduced numbers of EPCs in diabetes were most probably due to that diabetes strongly affects bone marrow (BM) structure and function [4]. Both in mice [4] and in humans [5], the diabetic BM is characterized by microangiopathy and alterations of the stem cell niche. Alessia et al. reported that in mice, type 1 diabetes induced a dysregulation of cytokines in the bone marrow plasma [6]. A very recent study of diabetic patients demonstrates a remarkable remodeling of BM from hip bones, consisting of decreased hematopoietic tissue,

fat deposition, and bone rarefaction [5]. Therefore, these studies led to the discovery that BM was the primary target of diabetes mellitus-induced damage. But until today, the diabetic bone marrow cells have remained a poorly explored cell type. Thus, it would be of sufficient importance to explore the differential gene expression profile to these cells on a genome scale.

In the present study, we compared bone marrow cells from type 2 diabetic mice and wild type mice by microarray-based gene expression profiling, and identified genes that were significantly changed. Focusing on biological processes of the up or down regulated genes will help to refine the mechanisms that are involved in the development of type 2 diabetes.

Methods

BM collection and RNA extraction

Eight-weeks-old BKS.Cg-+*Lepr*^{db}/+*Lepr*^{db}/Jcl (*db/db*) mice and BKS.Cg-*m*+/*m*+/Jcl (*m/m*) control mice were purchased from Clea Japan (Tokyo, Japan). All animals were housed in the animal facility of RIKEN Center for Developmental Biology on a 12:12-h light-dark cycle. The mice were provided free access to standard feed and tap water and were maintained at 25°C. For the qPCR validation, mice were obtained from Model Animal Research Center of Nanjing University and maintained in the animal facility of Soochow University. All animal studies were conducted in compliance with the Guidelines for the Care and Use of Research Animals established by RIKEN Center for Developmental Biology, Kobe, Japan and the ethical standards of the Ethic Committee of Soochow University. Db/db mice all have the typical syndromes of the type 2 diabetes. Body weight was measured and blood was collected from the tail vein at 10 weeks of age. Blood glucose was measured by the enzyme electrode method using a Free Style kit (Kissei Pharmaceutical, Nagano, Japan). After euthanizing mice with CO_2, the femorae and tibiae of both legs were immediately excised and bones were smashed with a mortar and a pestle. Then bone marrow cells were collected and placed on ice. RNA isolation was performed at room temperature using the RNeasy Mini Kit (Qiagen, Cat no. 74104) according to the manufacturer's instructions. Isolated RNA was snap-frozen and stored at -80°C for further use. RNA concentration was measured using a Nanodrop 1000 (Nanodrop Products, DE, USA), integrity was assessed using the BioRad Experion automated electrophoresis system (BioRad, CA, USA).

Microarray and bioinformatics analysis

RNA quality assessment and microarrays were performed by the Riken Center for Developmental Biology, Kobe, Japan. RNA integrity was confirmed using gel electrophoresis and Affymetrix Gene Chip Mouse Gene 1.0 ST Arrays were used. Microarray results were normalized using robust multi-array analysis (RMA) [7]. Differentially expressed genes (DE-genes) between diabetic and nondiabetic mice were identified using eBayes method [8]. Genes with p-value < 0.05 and fold-change (FC) > 1.5 were selected as significant differential expressed genes. The data obtained has been deposited in the NCBI Gene Expression Omnibus (GEO) database according to the MIAME guidelines (accession number GSE68619). Unsupervised hierarchical clustering was performed for differential expressed genes across all samples using the Euclidean distance method and the complete linkage method. Gene Ontology (GO) and pathway enrichment analysis was performed using DAVID [9]. The terms with p-value < 0.05 were selected. A user friendly plug-in for the Cytoscape called Enrichment Map was used to explore the relationships among gene sets that were enriched by the DE-genes [10]. PPI network of DEGs was constructed using Cytoscape MiMI plug-in [11]. It includes the DE-genes and their nearest neighbors.

Real-time PCR

CDNA was synthesised using PrimeScript™ RT reagent kit (TaKaRa, Cat. # RR037A) according to the manufacturer's protocol. Quantitative PCR (qPCR) was used to validate genes found to be differentially expressed on microarray. Glyceraldehydes 3-phosphate dehydrogenase (GAPDH) was used as the normalizing gene. Individual reactions (10 µl) contained 2×SYBR Mix (ABI, 4367660), forward and reverse primers (3 µM), 2 µl of cDNA and 2 µl of water. The PCR reactions were carried out in a ABI PRISM 7000 Sequence Detection System (Applied Biosystems, Foster City, CA, USA) followed by a dissociation curve. All samples were run in triplicate.

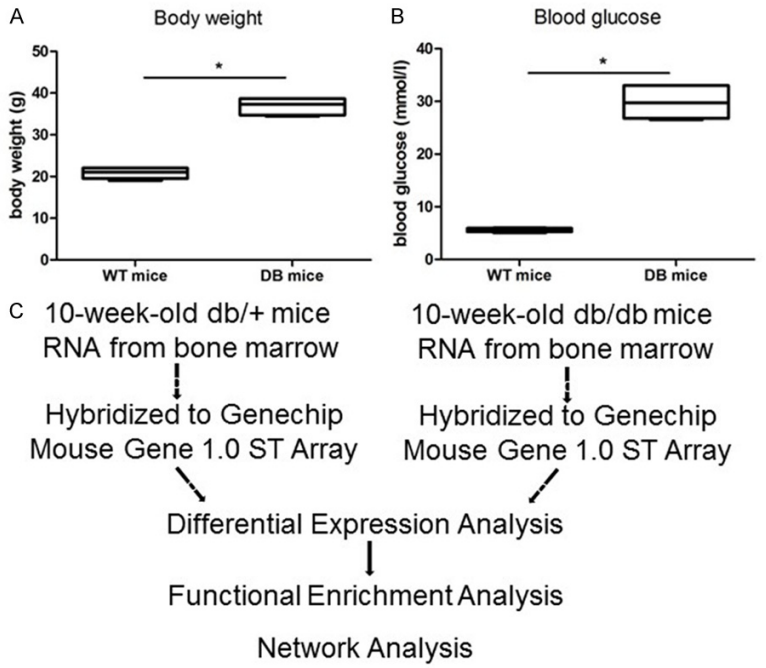

Figure 1. Body weight, blood glucose levels and transcriptional data analysis workflow. Body weight (A) and blood glucose levels (B) in non-diabetic (WT) and diabetic mice (DB) at 10 weeks of age. Asterisk (*) denotes statistical significance ($P < 0.05$). (C) RNA samples obtained from the bone marrow of db/db and db/+ mice were hybridized to Affymetrix GeneChip microarrays. Data quantified from scanned microarrays were analyzed to identify DEGs. Functional enrichment analysis of DEGs was performed to identify overrepresented biological categories and pathways. Network analysis identified functionally related subgroups of DEGs.

Cycle threshold (Ct) values for each sample were calculated using the ABI PRISM 7000 software. The relative expression ratio of each sample was calculated using the delta Ct method.

Statistical analysis

All values were presented as mean ± SEM. Comparisons between two groups were tested for significance via t-test. A *P* value less than 0.05 was considered statistically significant. The enrichment analysis was performed by DAVID. The terms in GO and KEGG with *p* value less than 0.05 were selected as significantly enriched terms. In DAVID, Fisher Exact is adopted to measure the gene-enrichment in annotation terms.

Results

Animal body weight and blood glucose levels

At the time of analysis, mice at 10 weeks of age had a body weight of 36.81 ± 1.99 g and 20.8 ± 1.3 g for diabetic and non-diabetic mice respectively (n = 5, P < 0.0001, **Figure 1A**). Mean blood glucose at 10 weeks of age was 29.86 ± 3.11 (26.5-33) mmol/l in diabetic and 5.58 ± 0.35 (5.1-6) mmol/l in nondiabetic animals (n = 5, P < 0.0001, **Figure 1B**).

Gene expression patterns in type 2 diabetic mice and wild type mice

Microarray expression analysis and comparison was performed on diabetic and wild type mice as **Figure 1C** outlined (n = 3). Totally, 95 genes were found to be differentially expressed between them (Supplemental File 1). Of these, 74 were down-regulated and 21 were up-regulated in the diabetic mice. Thirty one genes were reported to be related with diabetes mellitus, such as versican (Vcan), fibronectin, stefin A, Ifih1, Mx2, CXCL9 and CXCL10.

Then we performed hierarchical cluster analysis of 95 differential expressed genes (*p*-value < 0.05 and fold-change > 1.5) (**Figure 2**). It demonstrated that clustering of these genes distinguished diabetes from wild type mice. In addition, up-regulated Vcan and down-regulated Ifit3 were the top two differentially expressed genes with the highest fold change.

Gene enrichment analysis

To explore the function and annotation of the differential expressed genes, the GO and pathway enrichment analysis was performed by DAVID. GO covers three domains: biological process, cellular component and molecular function. As shown in **Figure 3** and Supplemental File 2, the significant enriched GO terms were grouped in the GO three domains. In biological process domain (red bar), 38 terms were significantly enriched and many of them related with immune response. Response to virus, defense response, immune response, inflammatory response, response to wounding and cellular defense response were related with

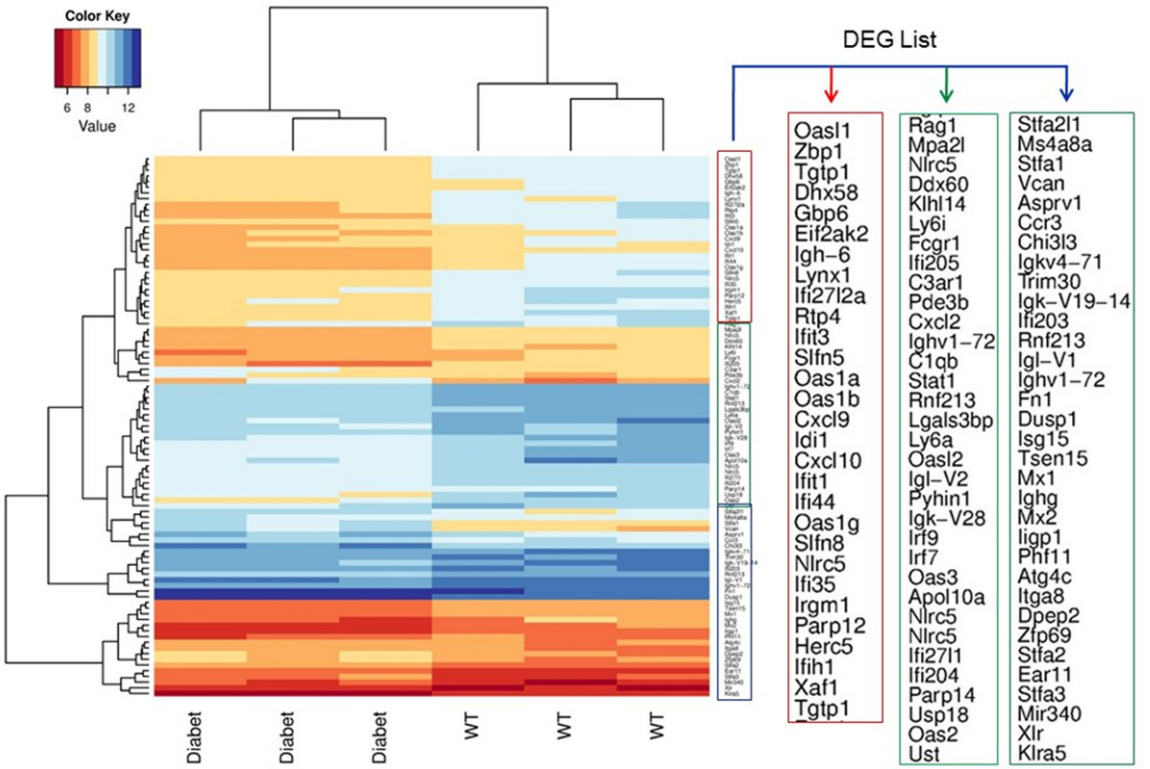

Figure 2. Cluster analysis of genes expression profiles of type 2 diabetic mice and wild type mice. High expression is indicated in blue, whereas low expression is coded in red. Each column corresponds to the expression profile of a mice sample, and each row corresponds to a gene. For clearance, the genes were showed in a magnified font by the right side.

development of diabetes. And chemotaxis had a close relationship with vasculogenesis. Ten terms of cellular component were significantly enriched (green bar). Meanwhile, in the molecular function domain, there were 8 terms enriched by the DE-genes (blue bar). The chemokine terms were significantly enriched.

At the same time, four pathways were significantly enriched by the 95 differentially expressed genes (**Figure 3** and Supplemental File 2), including RIG-I-like receptor signaling pathway, chemokine signaling pathway, Toll-like receptor signaling pathway and cytosolic DNA-sensing pathway. In line with the results of the GO analysis, chemokine signaling pathway was a most important pathway involved both in the development of diabetes and in the process of vasculogenesis.

Network analysis

The elucidation of biological concepts enriched with differentially expressed genes has become an integral part of the analysis and interpretation of genomic data. Experiment Map is a gene set relation mapping tool that identifies relationships (significant overlap) between gene sets in sources such as GO terms and Kyoto Encyclopedia of Genes and Genomes (KEGG) pathways. Experiment Map was used to analyze 95 DEGs annotated with the GO biological processes, GO cellular component, GO molecular function, KEGG pathways shown in Supplemental File 2. Relationships among significantly enriched terms by DAVID were visualized using Cytoscape (**Figure 4**). KEGG pathways with significant overlap with the terms included chemokine activity, taxis, immune response, chemokine receptor binding and chemotaxis (similarity coefficient > 0.7). Terms were grouped in two groups: immune response and protein binding.PPI network of DE-genes was constructed using Cytoscape MiMI plug-in. It included the DE-genes and their nearest neighbors (**Figure 5**). The hub Trim30 had the most neighbors.

Validation results of selected genes

To verify the type 2 diabetes-related molecular signature, genes were selected for validation by

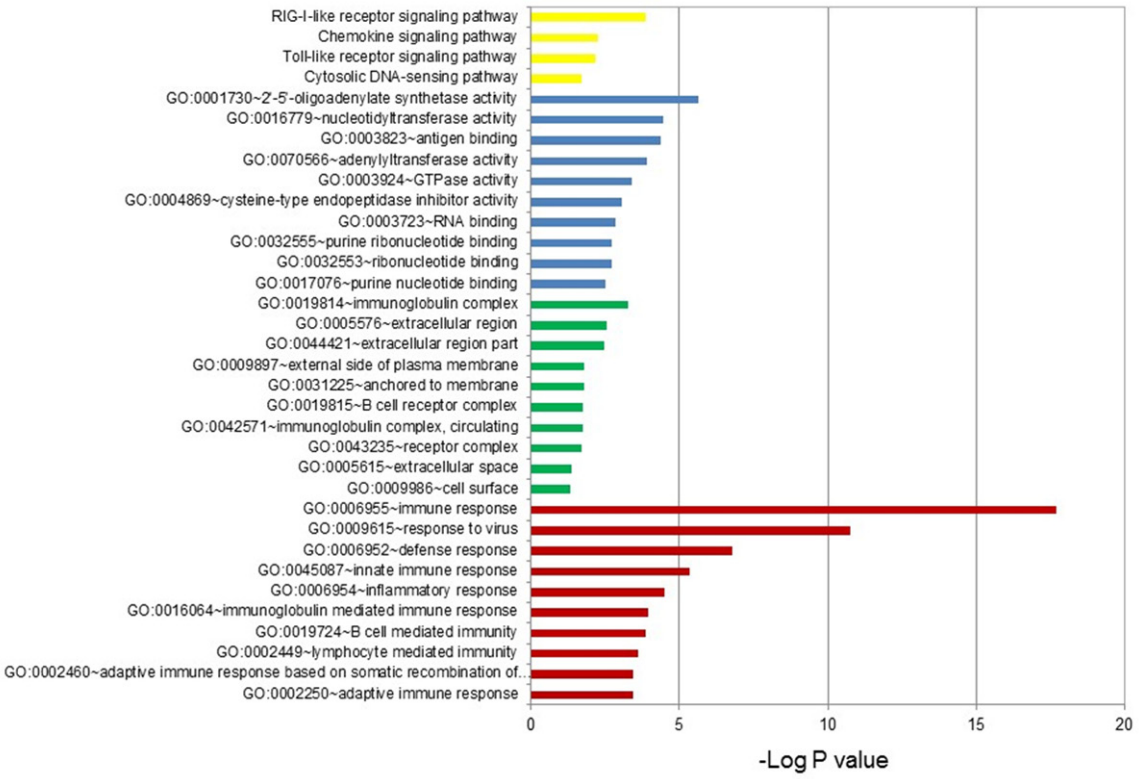

Figure 3. The significant enriched GO terms and pathways of type 2 diabetic mice and wild type mice. Biological process, cellular component and molecular function terms are marked by red bars, green bars and blue bars. KEGG pathways are marked by yellow bars.

qPCR (**Figure 6**). These genes were selected based on fold change differences, previous association with migration, and/or involvement in processes or pathways involved in vasculogenesis or diabetes. Totally 27 genes were validated by qPCR. As it turned out, all tested genes exhibited a high agreement with the microarray-generated gene expression data. The expressions of Ifi203, Ifi204, Ifi205, Ifi44, Ifit1, Ifit3, Irgm1, Ifi2712a, CXCL9, CXCL10 and Stat1 were significantly lower in type 2 diabetic mice compared to wild type mice (**Figure 6A-C**). Stefin A1, Stefin A2, Stfa2l1, Atg4c, Versican and Ear11 expressions were significantly higher in diabetic mice when compared to non-diabetic mice (**Figure 6D**).

Discussion

Diabetes mellitus causes a reduction of hematopoietic tissue, fat deposition, and microvascular rarefaction [5], especially when associated with critical limb ischemia. Moreover, diabetic BM cells show increased apoptosis, as assessed by immunohistochemistry and cell cycle analysis [12]. The appeal of investigating bone marrow change to elucidate dysfunctional stem cell microenvironment is that it is possible to figure out the most upstream mechanisms residing in the stem cell niche. Therefore, to gain a comprehensive understanding of bone marrow cells at the translational level, we performed gene expression arrays in type 2 diabetic mice and non-diabetic mice. It is the first study to measure and compare gene expression profiles in bone marrow cells of type 2 diabetic mice and non-diabetic mice to determine the mechanisms involved in the development of diabetes mellitus in these mice. This list included chemokines, interferon-inducible genes, genes related with angiogenesis and genes involved in extracellular environment, which provide important clues for further study.

Vascular complications, including microangiopathy and macroangiopathy, represent the most frequent and the most serious complications of diabetes mellitus. Our analyses revealed that angiogenesis-related genes (Stefin A and Pde3b) were upregulated in db/db bone mar-

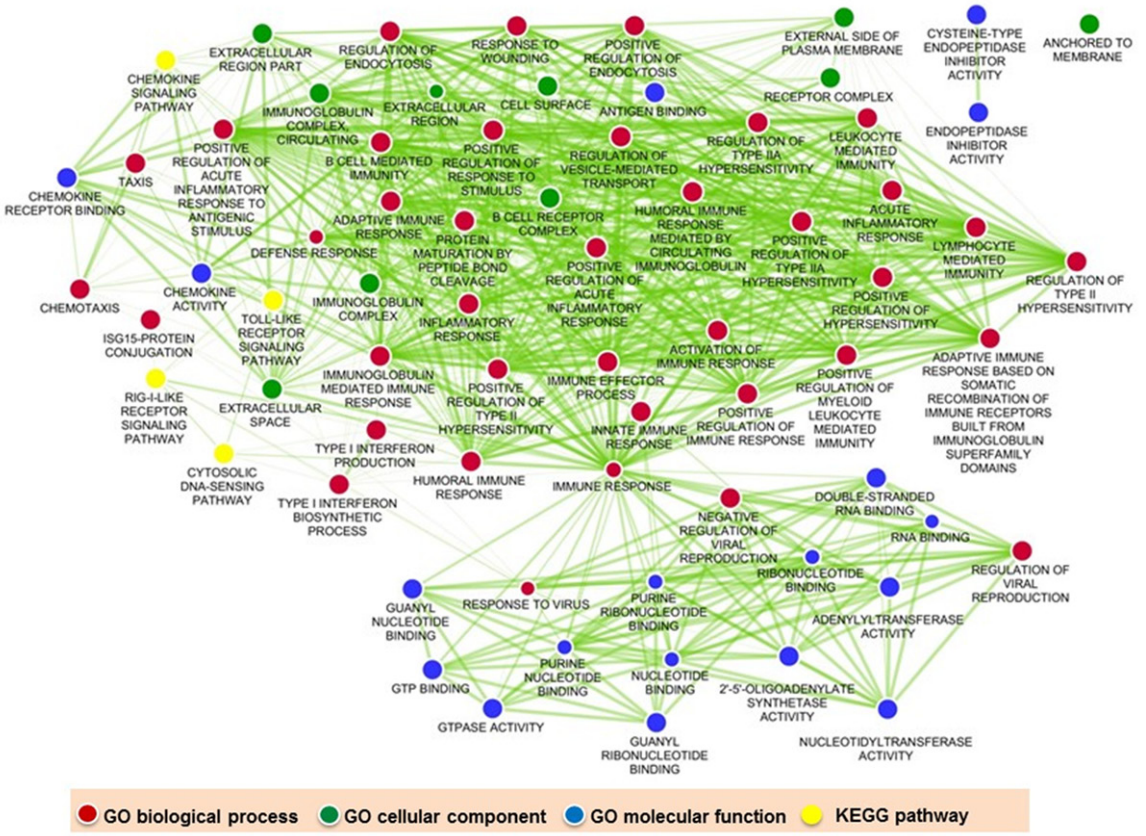

Figure 4. Enrichment map for DE-genes visualized in Cytoscape. Network depicts relationships and overlap among significantly overlapped terms (GO biological processes, GO cellular component, GO molecular function, KEGG pathways,) in the DE-genes. Node color represents term type, node size represents numbers of genes in the concept. Thickness of the edge represents gene overlap between terms. GO_BP: red, GO_CC: green, GO_MF: blue; KEGG pathway: yellow.

row. Stefin A is the intracellular inhibitor of the human lysosomal cysteine proteinases, cathepsins B, H and L [13]. Liu's group reports that stefin A plays an important role in the growth, angiogenesis, invasion, and metastasis of human esophageal squamous cell carcinoma cells [13]. Surprisingly, Stefin A strikingly inhibited matrigel invasion by 78% to 83% [14]. Considering that stefin A was increased in type 2 diabetic mice in this study, which is a most important difference between diabetic mice and non-diabetic mice, efforts are needed to elucidate the exact effect of stefin A in angiogenesis and their role in the regulating the vascular complications in diabetes mellitus. Another critical gene involved in angiogenesis is Pde3b. Pde3 is a phosphodiesterase, consists of two members, Pde3a and Pde3b, clinically significant because of its role in regulating heart muscle, vascular smooth muscle and platelet aggregation. Dr. Donald's group first reported that inhibition of Pde3b could promote tube formation of human arterial endothelial cells in 2011 [15]. Just very recently, Chung YW et al. has reported that targeted disruption of Pde3b protects murine heart from ischemia/reperfusion injury and defines a role for Pde3b against cardioprotection for the first time [16]. In line with our finding that Pde3b was increased in diabetes, we hypothesized Pde3b as a potent molecule involved in the impaired angiogenesis and cardiac functions in diabetes.

Dysregulation of chemotaxis is implicated in diabetic bone marrow [17], but the mechanism of its effect is not well understood. We observed downregulation of chemotatic factors (CXCL9 and CXCL10). As chemotatic factors, CXCL9 and CXCL10 not only can be involved in cell migration and invasion [18, 19], but also can promote mobilization of stem cells in bone mar-

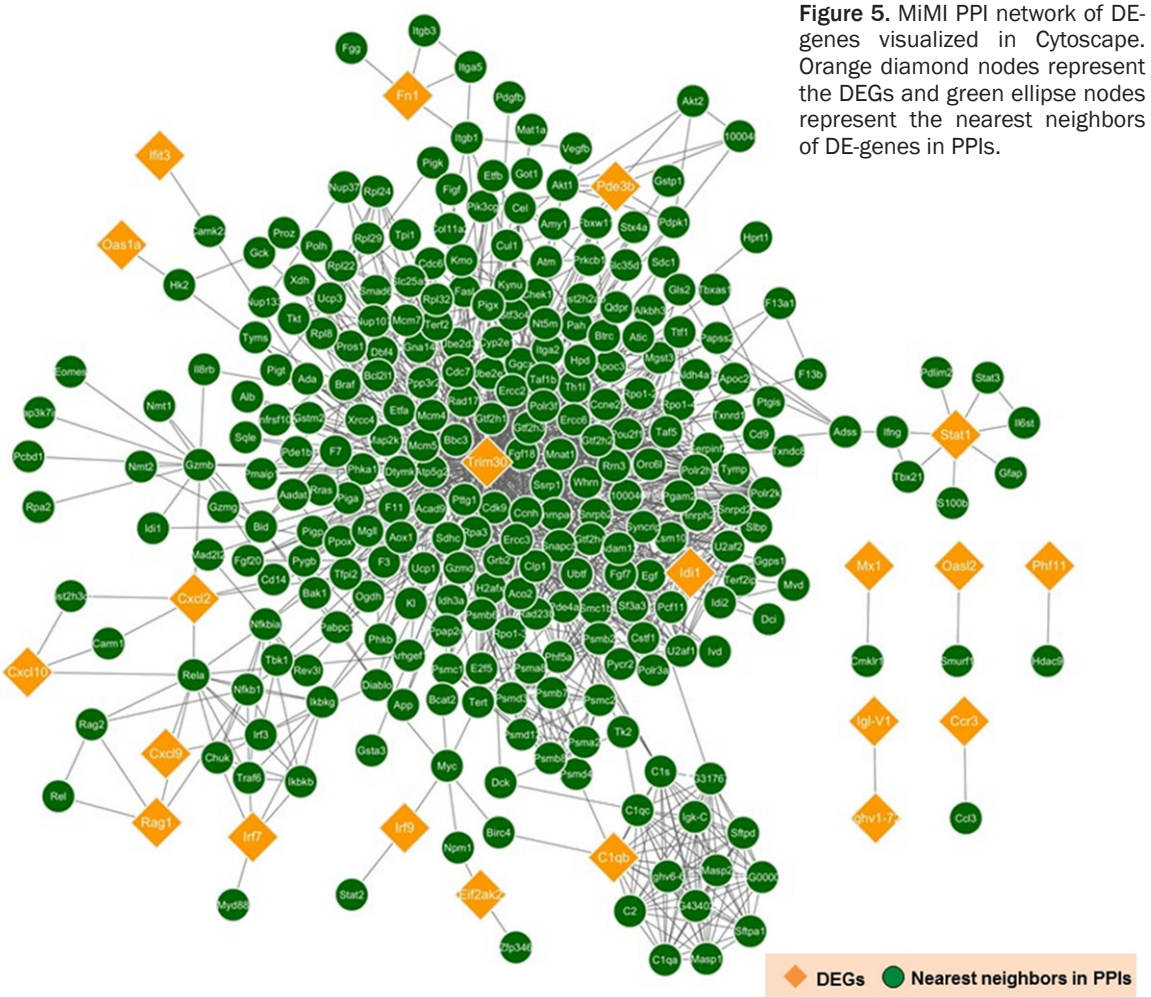

Figure 5. MiMI PPI network of DE-genes visualized in Cytoscape. Orange diamond nodes represent the DEGs and green ellipse nodes represent the nearest neighbors of DE-genes in PPIs.

row to ischemic sites [20]. Giselle et al. reported addition of exogenous CXCL9 increased MSC adherence, crawling and spreading on endothelial cells, in comparison to its absence, showing a significant effect of this chemokine [21]. Additionally, CXCL9/CXCR3 axis promotes efficient migration and activation in chronic lymphocytic leukemia cells and melanoma cells [18, 19]. In combination with the enrichment analysis results that fourteen of sixteen GO terms and all four pathways were enriched by the chemokine genes or chemokine receptor genes, we could hypothesize that decreased levels of CXCL9 and CXCL10 may result in reduced migration, invasion and decreased mobilization of stem cells in the bone marrow of diabetic mice upon stimuli such as ischemia, wound and inflammation, which needs further elucidation.

We have also shown that many interferon-related genes, like Ifi204, Ifi203, Ifih1, Ifit1, Ifit3, Ifi2712a, were significantly deduced in diabetic mice. Of these, Ifi204 is a most valuable gene for analyzing the functions of bone marrow cells. Ifi204 belongs to the interferon-inducible p200 family,which have been shown to be involved in the regulation of cell proliferation and differentiation [22]. A study by Liu et al. [23] showed that Ifi204 was sufficient to drive muscle differentiation by interacting with the muscle-specific transcription factor MyoD. Further studies showed that Ifi204 could interact with inhibition of differentiation (Id) proteins [24]. This is important because Id proteins bind to MyoD and other myogenic proteins and thus block their ability to activate transcription of the genes necessary for muscle cell maturation; so by releasing the inhibition of Id proteins to MyoD, Ifi204 may promote muscle differentiation [25]. By qPCR validation, we confirmed down-regulation of Ifi204 and up-regulation of Id2 in diabete BM cells (**Figure 6A** and **6E**), which could be the intrinsic factors that inhibit

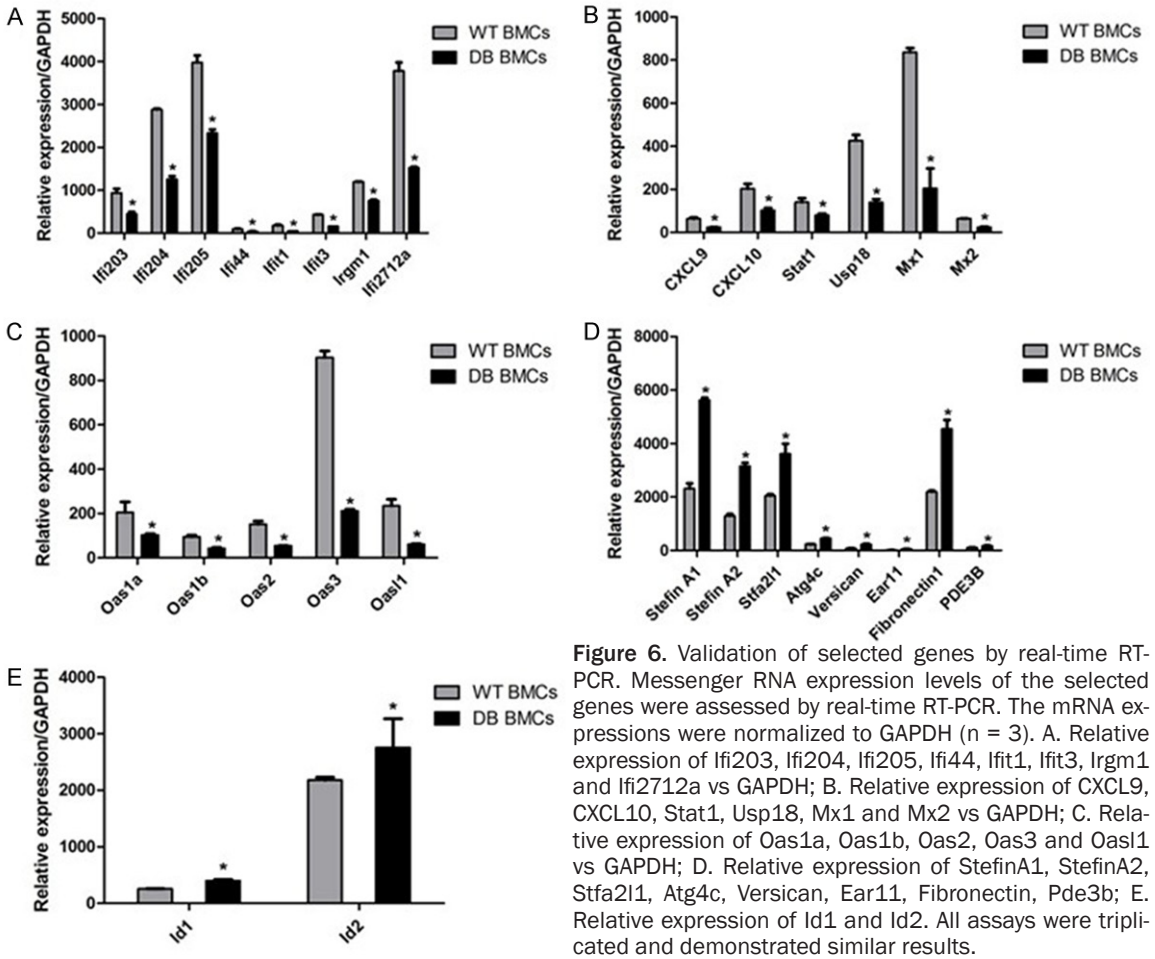

Figure 6. Validation of selected genes by real-time RT-PCR. Messenger RNA expression levels of the selected genes were assessed by real-time RT-PCR. The mRNA expressions were normalized to GAPDH (n = 3). A. Relative expression of Ifi203, Ifi204, Ifi205, Ifi44, Ifit1, Ifit3, Irgm1 and Ifi2712a vs GAPDH; B. Relative expression of CXCL9, CXCL10, Stat1, Usp18, Mx1 and Mx2 vs GAPDH; C. Relative expression of Oas1a, Oas1b, Oas2, Oas3 and Oasl1 vs GAPDH; D. Relative expression of StefinA1, StefinA2, Stfa2l1, Atg4c, Versican, Ear11, Fibronectin, Pde3b; E. Relative expression of Id1 and Id2. All assays were triplicated and demonstrated similar results.

cardiac muscle differentiation and lead to the progression of diabetic cardiomyopathy.

The extracellular matrix components are closely correlated with the progression of diabetes and hyperlipidemia [26]. Fibronectin 1, which was identified up-regulated in our study, has been reported to be a potential pregnancy-specific biomarker for early identification of women at risk for gestational diabetes [27]. Versican, one of the top differentially expressed genes with the highest fold change in this study, has also been reported to be up-regulated in bones of diabetes mellitus type 2 patients by A. T. Haug et al. [28]. Along with the analysis that GO cellular component, for example extracellular space and extracellular region, was modulated by db/db bone marrow, our data indicated that the extracellular environment of diabetes mellitus might be more intimately correlated with respect to the development of diabetes mellitus and its complications.

To explore the role of differential expressed genes in type 2 diabetes from network view and system level, we also performed the enrichment analysis and network analysis of these genes. The enrichment analysis results showed that most of the significantly enriched terms could be grouped into two types: immune response related and chemokines related. Moreover, in the enrichment map of significantly enriched terms, immune response occupied an important position which had the most overlaps with other terms. Chemokines also played a critical role in the development of diabetes. Studies reported that interference with the CXCL10/CXCR3 axis can be an effective strategy to suppress diabetes onset both in the malignant phase [29], i.e. the active disease phase, and in the benign phase, i.e. the less active phase. At last, we also constructed the PPI network by MiMI which consists of the DE-genes and their nearest neighbors. Trim30 had most neighbors and it may play a role in the

disease. Actually, trim 30 negatively regulates TLR-mediated NF-kappaB activation, by which cells keep the inflammatory response in check to avoid excessive harmful immune response triggered by NF-kappaB [30].

In conclusion, gene expression changes in the bone marrow suggest roles of multiple etiological factors in the development of diabetes and its complications. Our findings support the new molecular mechanisms that may account for impaired angiogenesis and mobilization of stem cells in diabetes mellitus. In addition, our analyses reveal that chemokine signaling pathway is a most important pathway involved both in the development of diabetes and in the process of vasculogenesis. Further investigation into the signaling pathways is likely to provide more insights into diabetes-induced bone marrow damage.

Acknowledgements

This work was supported by research funding from the Foundation of Biomedical Research and Innovation of Kobe, Japan, the National Natural Science Foundation of China (No. 81400199) and Suzhou Municipal Science and Technology Project of China (No. SYS201414). The authors would like to thank the animal facility of *RIKEN Center for Developmental Biology* and the animal center of Soochow University for providing the space to perform animal surgery.

Disclosure of conflict of interest

None.

Address correspondence to: Dr. Takayuki Asahara, Department of Regenerative Medicine, Division of Basic Clinical Science, Tokai University School of Medicine, Shimokasuya, Isehara, Kanagawa 259-1143, Japan. Tel: +81-78-304-5772; Fax: +81-78-304-5263; E-mail: asa777@is.icc.u-tokai.ac.jp; Zhenya Shen, Department of Cardiovascular Surgery, The First Affiliated Hospital of Soochow University, 188, Shizi Street, Suzhou 215006, China. E-mail: uuzyshen@aliyun.com

References

[1] Xu J and Zou MH. Molecular insights and therapeutic targets for diabetic endothelial dysfunction. Circulation 2009; 120: 1266-1286.

[2] Ii M, Takenaka H, Asai J, Ibusuki K, Mizukami Y, Maruyama K, Yoon YS, Wecker A, Luedemann C, Eaton E, Silver M, Thorne T and Losordo DW. Endothelial progenitor thrombospondin-1 mediates diabetes-induced delay in reendothelialization following arterial injury. Circ Res 2006; 98: 697-704.

[3] Sorrentino SA, Bahlmann FH, Besler C, Muller M, Schulz S, Kirchhoff N, Doerries C, Horvath T, Limbourg A, Limbourg F, Fliser D, Haller H, Drexler H and Landmesser U. Oxidant stress impairs in vivo reendothelialization capacity of endothelial progenitor cells from patients with type 2 diabetes mellitus: restoration by the peroxisome proliferator-activated receptor-gamma agonist rosiglitazone. Circulation 2007; 116: 163-173.

[4] Oikawa A, Siragusa M, Quaini F, Mangialardi G, Katare RG, Caporali A, van Buul JD, van Alphen FP, Graiani G, Spinetti G, Kraenkel N, Prezioso L, Emanueli C and Madeddu P. Diabetes mellitus induces bone marrow microangiopathy. Arterioscler Thromb Vasc Biol 30: 498-508.

[5] Spinetti G, Cordella D, Fortunato O, Sangalli E, Losa S, Gotti A, Carnelli F, Rosa F, Riboldi S, Sessa F, Avolio E, Beltrami AP, Emanueli C and Madeddu P. Global remodeling of the vascular stem cell niche in bone marrow of diabetic patients: implication of the microRNA-155/FOXO3a signaling pathway. Circ Res 112: 510-522.

[6] Orlandi A, Chavakis E, Seeger F, Tjwa M, Zeiher AM and Dimmeler S. Long-term diabetes impairs repopulation of hematopoietic progenitor cells and dysregulates the cytokine expression in the bone marrow microenvironment in mice. Basic Res Cardiol 105: 703-712.

[7] Irizarry RA, Hobbs B, Collin F, Beazer-Barclay YD, Antonellis KJ, Scherf U and Speed TP. Exploration, normalization, and summaries of high density oligonucleotide array probe level data. Biostatistics 2003; 4: 249-264.

[8] Smyth GK. Linear models and empirical bayes methods for assessing differential expression in microarray experiments. Stat Appl Genet Mol Biol 2004; 3: Article3.

[9] Huang da W, Sherman BT and Lempicki RA. Systematic and integrative analysis of large gene lists using DAVID bioinformatics resources. Nat Protoc 2009; 4: 44-57.

[10] Merico D, Isserlin R, Stueker O, Emili A and Bader GD. Enrichment map: a network-based method for gene-set enrichment visualization and interpretation. PLoS One 2010; 5: e13984.

[11] Gao J, Ade AS, Tarcea VG, Weymouth TE, Mirel BR, Jagadish HV and States DJ. Integrating and annotating the interactome using the MiMI plugin for cytoscape. Bioinformatics 2009; 25: 137-138.

[12] Westerweel PE, Teraa M, Rafii S, Jaspers JE, White IA, Hooper AT, Doevendans PA and Ver-

haar MC. Impaired endothelial progenitor cell mobilization and dysfunctional bone marrow stroma in diabetes mellitus. PLoS One 8: e60357.
[13] Li W, Ding F, Zhang L, Liu Z, Wu Y, Luo A, Wu M, Wang M and Zhan Q. Overexpression of stefin A in human esophageal squamous cell carcinoma cells inhibits tumor cell growth, angiogenesis, invasion, and metastasis. Clin Cancer Res 2005; 11: 8753-8762.
[14] Chang SH, Kanasaki K, Gocheva V, Blum G, Harper J, Moses MA, Shih SC, Nagy JA, Joyce J, Bogyo M, Kalluri R and Dvorak HF. VEGF-A induces angiogenesis by perturbing the cathepsin-cysteine protease inhibitor balance in venules, causing basement membrane degradation and mother vessel formation. Cancer Res 2009; 69: 4537-4544.
[15] Wilson LS, Baillie GS, Pritchard LM, Umana B, Terrin A, Zaccolo M, Houslay MD and Maurice DH. A phosphodiesterase 3B-based signaling complex integrates exchange protein activated by cAMP 1 and phosphatidylinositol 3-kinase signals in human arterial endothelial cells. J Biol Chem 286: 16285-16296.
[16] Chung YW, Lagranha C, Chen Y, Sun J, Tong G, Hockman SC, Ahmad F, Esfahani SG, Bae DH, Polidovitch N, Wu J, Rhee DK, Lee BS, Gucek M, Daniels MP, Brantner CA, Backx PH, Murphy E and Manganiello VC. Targeted disruption of PDE3B, but not PDE3A, protects murine heart from ischemia/reperfusion injury. Proc Natl Acad Sci U S A 2015; 112: E2253-2262.
[17] Juarez JG, Thien M, Dela Pena A, Baraz R, Bradstock KF and Bendall LJ. CXCR4 mediates the homing of B cell progenitor acute lymphoblastic leukaemia cells to the bone marrow via activation of p38MAPK. Br J Haematol 2009; 145: 491-499.
[18] Amatschek S, Lucas R, Eger A, Pflueger M, Hundsberger H, Knoll C, Grosse-Kracht S, Schuett W, Koszik F, Maurer D and Wiesner C. CXCL9 induces chemotaxis, chemorepulsion and endothelial barrier disruption through CXCR3-mediated activation of melanoma cells. Br J Cancer 104: 469-479.
[19] Mahadevan D, Choi J, Cooke L, Simons B, Riley C, Klinkhammer T, Sud R, Maddipoti S, Hehn S, Garewal H and Spier C. Gene Expression and Serum Cytokine Profiling of Low Stage CLL Identify WNT/PCP, Flt-3L/Flt-3 and CXCL9/CXCR3 as Regulators of Cell Proliferation, Survival and Migration. Hum Genomics Proteomics 2009; 2009: 453634.
[20] Jinquan T, Anting L, Jacobi HH, Glue C, Jing C, Ryder LP, Madsen HO, Svejgaard A, Skov PS, Malling HJ and Poulsen LK. CXCR3 expression on CD34(+) hemopoietic progenitors induced by granulocyte-macrophage colony-stimulating factor: II. Signaling pathways involved. J Immunol 2001; 167: 4405-4413.
[21] Chamberlain G, Smith H, Rainger GE and Middleton J. Mesenchymal stem cells exhibit firm adhesion, crawling, spreading and transmigration across aortic endothelial cells: effects of chemokines and shear. PLoS One 6: e25663.
[22] Asefa B, Klarmann KD, Copeland NG, Gilbert DJ, Jenkins NA and Keller JR. The interferon-inducible p200 family of proteins: a perspective on their roles in cell cycle regulation and differentiation. Blood Cells Mol Dis 2004; 32: 155-167.
[23] Liu C, Wang H, Zhao Z, Yu S, Lu YB, Meyer J, Chatterjee G, Deschamps S, Roe BA and Lengyel P. MyoD-dependent induction during myoblast differentiation of p204, a protein also inducible by interferon. Mol Cell Biol 2000; 20: 7024-7036.
[24] D'Souza S, Xin H, Walter S and Choubey D. The gene encoding p202, an interferon-inducible negative regulator of the p53 tumor suppressor, is a target of p53-mediated transcriptional repression. J Biol Chem 2001; 276: 298-305.
[25] Liu CJ, Ding B, Wang H and Lengyel P. The MyoD-inducible p204 protein overcomes the inhibition of myoblast differentiation by Id proteins. Mol Cell Biol 2002; 22: 2893-2905.
[26] McDonald TO, Gerrity RG, Jen C, Chen HJ, Wark K, Wight TN, Chait A and O'Brien KD. Diabetes and arterial extracellular matrix changes in a porcine model of atherosclerosis. J Histochem Cytochem 2007; 55: 1149-1157.
[27] Rasanen JP, Snyder CK, Rao PV, Mihalache R, Heinonen S, Gravett MG, Roberts CT Jr and Nagalla SR. Glycosylated fibronectin as a first-trimester biomarker for prediction of gestational diabetes. Obstet Gynecol 2013; 122: 586-594.
[28] Haug AT, Braun KF, Ehnert S, Mayer L, Stockle U, Nussler AK, Pscherer S and Freude T. Gene expression changes in cancellous bone of type 2 diabetics: a biomolecular basis for diabetic bone disease. Langenbecks Arch Surg 399: 639-647.
[29] Yamada S, Irie J, Shimada A, Kodama K, Morimoto J, Suzuki R, Oikawa Y and Saruta T. Assessment of beta cell mass and oxidative peritoneal exudate cells in murine type 1 diabetes using adoptive transfer system. Autoimmunity 2003; 36: 63-70.
[30] Hu Y, Mao K, Zeng Y, Chen S, Tao Z, Yang C, Sun S, Wu X, Meng G and Sun B. Tripartite-motif protein 30 negatively regulates NLRP3 inflammasome activation by modulating reactive oxygen species production. J Immunol 2010; 185: 7699-7705.

Supplemental File 1. Up or down-regulated genes in diabetes mellitus

Gene Name	Gene Symbol	Down/ Up	Fold change	*P*-value
Interferon-induced protein with tetratricopeptide repeats 3	Ifit3	Down	3.430580108	2.53629E-05
Receptor transporter protein 4	Rtp4	Down	3.18830554	0.000178558
Interferon, alpha-inducible protein 27 like 2A	Ifi27l2a	Down	3.07453113	4.31261E-05
2'-5' oligoadenylate synthetase 1G	Oas1g	Down	2.974592243	9.87634E-05
Interferon activated gene 205	Ifi205	Down	2.880506521	9.33886E-07
Interferon-induced protein with tetratricopeptide repeats 1	Ifit1	Down	2.815175026	0.000752459
2'-5' oligoadenylate synthetase 2	Oas2	Down	2.809943535	6.9792E-05
Ubiquitin specific peptidase 18	Usp18	Down	2.676163636	8.90177E-05
Interferon-induced protein 44	Ifi44	Down	2.664844836	0.000347971
2'-5' oligoadenylate synthetase-like 2	Oasl2	Down	2.549076994	0.000165562
Apolipoprotein L 10a	Apol10a	Down	2.4731789	0.018592537
Interferon regulatory factor 7	Irf7	Down	2.4591308	0.000253426
XIAP associated factor 1	Xaf1	Down	2.398321187	0.000129975
Schlafen 5	Slfn5	Down	2.386452914	2.97058E-05
2'-5' oligoadenylate synthetase 3	Oas3	Down	2.205585853	0.000975179
Lymphocyte antigen 6 complex, locus A	Ly6a	Down	2.091394934	0.000319808
Chemokine (C-X-C motif) ligand 9	Cxcl9	Down	2.090275418	2.24041E-05
T-cell specific GTPase 1	Tgtp1	Down	2.075285406	7.23507E-05
T-cell specific GTPase 1	Tgtp1	Down	2.050281827	6.29508E-05
Poly (ADP-ribose) polymerase family, member 12	Parp12	Down	2.034216889	0.000161166
2'-5' oligoadenylate synthetase 1A	Oas1a	Down	1.991160818	4.17808E-05
Uronyl-2-sulfotransferase	Ust	Down	1.983678104	0.028889838
Z-DNA binding protein 1	Zbp1	Down	1.955645249	6.39428E-05
Immunoglobulin heavy chain (gamma polypeptide)	Ighg	Down	1.945698762	0.029304469
Interferon activated gene 204	Ifi204	Down	1.925535087	4.71121E-06
2'-5' oligoadenylate synthetase-like 1	Oasl1	Down	1.912831712	0.000122499
Myxovirus (influenza virus) resistance 1	Mx1	Down	1.897583253	7.49307E-05
Immunity-related GTPase family M member 1	Irgm1	Down	1.866577889	1.53511E-05
Lectin, galactoside-binding, soluble, 3 binding protein	Lgals3bp	Down	1.818654495	0.000917614
Interferon inducible GTPase 1	Iigp1	Down	1.787387941	0.00036949
Interferon, alpha-inducible protein 27 like 1	Ifi27l1	Down	1.77302188	0.000452869
Schlafen 8	Slfn8	Down	1.7706938	0.000335985
DEXH (Asp-Glu-X-His) box polypeptide 58	Dhx58	Down	1.753154393	9.3547E-05
Lymphocyte antigen 6 complex, locus I	Ly6i	Down	1.745939679	0.006067385
2'-5' oligoadenylate synthetase 1B	Oas1b	Down	1.744272373	0.00049097
Chemokine (C-X-C motif) ligand 10	Cxcl10	Down	1.735698077	0.000289555
Immunoglobulin kappa chain variable 28 (V28)	Igk-V28	Down	1.733058863	0.005477313
Myxovirus (influenza virus) resistance 2	Mx2	Down	1.73189588	0.004665008
ISG15 ubiquitin-like modifier	Isg15	Down	1.725762565	0.003391887
Interferon regulatory factor 9	Irf9	Down	1.715655577	0.000126139
Immunoglobulin heavy chain 6 (heavy chain of IgM)	Igh-6	Down	1.708839158	0.011445708
Interferon induced with helicase C domain 1	Ifih1	Down	1.692588103	0.006821049
Killer cell lectin-like receptor, subfamily A, member 5	Klra5	Down	1.686062268	0.00849871
Hect domain and RLD 5	Herc5	Down	1.666766081	0.012698304
Ring finger protein 213	Rnf213	Down	1.65770833	6.33087E-05
Immunoglobulin kappa chain variable 19 (V19)-14	Igk-V19-14	Down	1.651078482	0.031083764
NLR family, CARD domain containing 5	Nlrc5	Down	1.625257526	0.002139962

Eukaryotic translation initiation factor 2-alpha kinase 2	Eif2ak2	Down	1.625090652	0.001763502
Ring finger protein 213	Rnf213	Down	1.609621504	7.05236E-05
Fc receptor, IgG, high affinity I	Fcgr1	Down	1.59777191	4.95971E-05
Immunoglobulin heavy variable V1-72	Ighv1-72	Down	1.593937459	0.000933707
DEAD (Asp-Glu-Ala-Asp) box polypeptide 60	Ddx60	Down	1.589723868	0.002409781
Guanylate binding protein 6	Gbp6	Down	1.589452418	0.000152
Poly (ADP-ribose) polymerase family, member 14	Parp14	Down	1.586836613	0.00031905
Immunoglobulin lambda chain, variable 2	Igl-V2	Down	1.579397418	0.011554449
Ly6/neurotoxin 1	Lynx1	Down	1.573366409	0.009732822
Macrophage activation 2 like	Mpa2l	Down	1.570147449	0.002848337
NLR family, CARD domain containing 5	Nlrc5	Down	1.568152269	0.005240031
NLR family, CARD domain containing 5	Nlrc5	Down	1.564651762	0.001394554
Interferon activated gene 203	Ifi203	Down	1.563467946	0.007092067
NLR family, CARD domain containing 5	Nlrc5	Down	1.560593301	0.00105924
Pyrin and HIN domain family, member 1	Pyhin1	Down	1.557574297	0.029741803
Interferon-induced protein 35	Ifi35	Down	1.55383272	0.000225551
Immunoglobulin lambda chain, variable 1	Igl-V1	Down	1.553728983	0.000168954
Immunoglobulin kappa chain variable 4-71	Igkv4-71	Down	1.553721793	0.009490185
Tripartite motif-containing 30	Trim30	Down	1.553331899	0.00089504
Immunoglobulin heavy variable V1-72	Ighv1-72	Down	1.540238417	0.002023451
Complement component 1, q subcomponent, beta polypeptide	C1qb	Down	1.532992682	0.00233968
Isopentenyl-diphosphate delta isomerase	Idi1	Down	1.530750059	0.047518798
tRNA splicing endonuclease 15 homolog (S. cerevisiae)	Tsen15	Down	1.523681234	0.00458946
Recombination activating gene 1	Rag1	Down	1.5173119	0.037571819
PHD finger protein 11	Phf11	Down	1.510412292	0.002589074
Signal transducer and activator of transcription 1	Stat1	Down	1.508767762	0.000229176
Kelch-like 14 (Drosophila)	Klhl14	Down	1.508102842	0.026075432
Phosphodiesterase 3B, cGMP-inhibited	Pde3b	Up	1.524645774	0.004418591
microRNA 340	Mir340	Up	1.545616852	0.015350702
Integrin alpha 8	Itga8	Up	1.561448395	0.00016175
Chemokine (C-C motif) receptor 3	Ccr3	Up	1.56434771	0.001020405
Fibronectin 1	Fn1	Up	1.5705978	0.002357428
Membrane-spanning 4-domains, subfamily A, member 8A	Ms4a8a	Up	1.585162312	0.00360887
Complement component 3a receptor 1	C3ar1	Up	1.606604295	0.006005586
Zinc finger protein 69	Zfp69	Up	1.61974275	0.022161332
Stefin A3	Stfa3	Up	1.625055739	0.011497032
Dipeptidase 2	Dpep2	Up	1.657306036	0.000390795
Autophagy-related 4C (yeast)	Atg4c	Up	1.676452809	3.49174E-05
Dual specificity phosphatase 1	Dusp1	Up	1.698614559	0.000264743
X-linked lymphocyte-regulated complex	Xlr	Up	1.812610095	0.026239367
Eosinophil-associated, ribonuclease A family, member 11	Ear11	Up	1.820284803	4.33046E-05
Aspartic peptidase, retroviral-like 1	Asprv1	Up	1.890548426	0.002544873
Chitinase 3-like 3	Chi3l3	Up	1.951383813	0.000185756
Stefin A2 like 1	Stfa2l1	Up	2.074408986	0.002030789
Chemokine (C-X-C motif) ligand 2	Cxcl2	Up	2.260793182	0.038492977
Stefin A2	Stfa2	Up	2.331382698	0.000387231
Stefin A1	Stfa1	Up	2.482219823	9.03117E-06
Versican	Vcan	Up	2.703821261	0.000655022

Supplemental File 2. Gene Ontology and KEGG pathways that DEGs are involved in

Category	Term	Number of genes	*P*-Value	Genes	Fold Enrichment
GO_BP	GO:0006955~immune response	23	1.99E-18	GBP6, IFIH1, IRGM1, CXCL2, CXCL9, OAS3, IGH-6, OAS2, FCGR1, CXCL10, IGHG, C1QB, IRF7, OASL2, OASL1, OAS1B, TGTP1, OAS1A, MX1, MPA2L, OAS1G, MX2, DHX58	11.84880194
GO_BP	GO:0009615~response to virus	10	1.70E-11	IFIH1, ISG15, IFI-27L2A, IRF7, OAS1B, TGTP1, OAS1A, MX1, EIF2AK2, MX2	31.92669173
GO_BP	GO:0006952~defense response	13	1.72E-07	IGHG, C1QB, IFIH1, IRGM1, CXCL2, CXCL9, CHI3L3, MX1, FCGR1, MX2, DHX58, FN1, CXCL10	7.040975765
GO_BP	GO:0045087~innate immune response	7	4.39E-06	C1QB, IFIH1, IRGM1, MX1, MX2, FCGR1, DHX58	15.87383178
GO_BP	GO:0006954~inflammatory response	8	3.21E-05	IGHG, C1QB, CXCL2, CXCL9, CHI3L3, FCGR1, FN1, CXCL10	8.627301587
GO_BP	GO:0016064~immunoglobulin mediated immune response	5	1.20E-04	IGHG, C1QB, IRF7, IGH-6, FCGR1	19.25736961
GO_BP	GO:0019724~B cell mediated immunity	5	1.35E-04	IGHG, C1QB, IRF7, IGH-6, FCGR1	18.66483516
GO_BP	GO:0002449~lymphocyte mediated immunity	5	2.48E-04	IGHG, C1QB, IRF7, IGH-6, FCGR1	15.96334586
GO_BP	GO:0002250~adaptive immune response	5	3.65E-04	IGHG, C1QB, IRF7, IGH-6, FCGR1	14.44302721
GO_BP	GO:0002460~adaptive immune response based on somatic recombination of immune receptors built from immunoglobulin superfamily domains	5	3.65E-04	IGHG, C1QB, IRF7, IGH-6, FCGR1	14.44302721
GO_BP	GO:0002443~leukocyte mediated immunity	5	4.55E-04	IGHG, C1QB, IRF7, IGH-6, FCGR1	13.63162119
GO_BP	GO:0009611~response to wounding	8	4.72E-04	IGHG, C1QB, CXCL2, CXCL9, CHI3L3, FCGR1, FN1, CXCL10	5.594071634
GO_BP	GO:0002252~immune effector process	5	0.00166835	IGHG, C1QB, IRF7, IGH-6, FCGR1	9.628684807
GO_BP	GO:0002526~acute inflammatory response	4	0.00428391	IGHG, C1QB, FCGR1, FN1	11.98236332
GO_BP	GO:0048525~negative regulation of viral reproduction	2	0.00807929	OAS1B, OAS1A	242.6428571
GO_BP	GO:0045807~positive regulation of endocytosis	3	0.00830622	IGHG, IGH-6, FCGR1	21.40966387
GO_BP	GO:0002455~humoral immune response mediated by circulating immunoglobulin	3	0.00878692	IGHG, C1QB, IGH-6	20.79795918
GO_BP	GO:0042330~taxis	4	0.00973563	C3AR1, CCR3, CXCL2, CXCL10	8.904325033
GO_BP	GO:0006935~chemotaxis	4	0.00973563	C3AR1, CCR3, CXCL2, CXCL10	8.904325033
GO_BP	GO:0032020~ISG15-protein conjugation	2	0.01609448	USP18, ISG15	121.3214286
GO_BP	GO:0050778~positive regulation of immune response	4	0.01761864	IGHG, C1QB, IGH-6, FCGR1	7.136554622
GO_BP	GO:0030100~regulation of endocytosis	3	0.01874367	IGHG, IGH-6, FCGR1	13.99862637
GO_BP	GO:0032606~type I interferon production	2	0.0200782	IRF9, IRF7	97.05714286
GO_BP	GO:0045351~type I interferon biosynthetic process	2	0.0200782	IRF9, IRF7	97.05714286
GO_BP	GO:0006959~humoral immune response	3	0.02012429	IGHG, C1QB, IGH-6	13.48015873
GO_BP	GO:0051605~protein maturation by peptide bond cleavage	3	0.02843813	IGHG, C1QB, ASPRV1	11.1989011

GO_BP	GO:0002888~positive regulation of myeloid leukocyte mediated immunity	2	0.03193457	IGHG, FCGR1	60.66071429
GO_BP	GO:0002892~regulation of type II hypersensitivity	2	0.03193457	IGHG, FCGR1	60.66071429
GO_BP	GO:0002894~positive regulation of type II hypersensitivity	2	0.03193457	IGHG, FCGR1	60.66071429
GO_BP	GO:0050792~regulation of viral reproduction	2	0.03193457	OAS1B, OAS1A	60.66071429
GO_BP	GO:0001798~positive regulation of type IIa hypersensitivity	2	0.03193457	IGHG, FCGR1	60.66071429
GO_BP	GO:0001796~regulation of type IIa hypersensitivity	2	0.03193457	IGHG, FCGR1	60.66071429
GO_BP	GO:0048584~positive regulation of response to stimulus	4	0.03940179	IGHG, C1QB, IGH-6, FCGR1	5.21812596
GO_BP	GO:0002866~positive regulation of acute inflammatory response to antigenic stimulus	2	0.03976045	IGHG, FCGR1	48.52857143
GO_BP	GO:0002885~positive regulation of hypersensitivity	2	0.03976045	IGHG, FCGR1	48.52857143
GO_BP	GO:0002675~positive regulation of acute inflammatory response	2	0.04365007	IGHG, FCGR1	44.11688312
GO_BP	GO:0060627~regulation of vesicle-mediated transport	3	0.04443754	IGHG, IGH-6, FCGR1	8.770223752
GO_BP	GO:0002253~activation of immune response	3	0.04736535	IGHG, C1QB, IGH-6	8.464285714
GO_CC	GO:0019814~immunoglobulin complex	3	5.17E-04	IGHG, IGH-6, IGL-V1	84.86877828
GO_CC	GO:0005576~extracellular region	12	0.0028289	IGHG, C1QB, LGALS3BP, ISG15, CXCL2, CXCL9, APOL10A, VCAN, CHI3L3, IGH-6, FN1, CXCL10	2.626890756
GO_CC	GO:0044421~extracellular region part	8	0.0035105	IGHG, LGALS3BP, CXCL2, CXCL9, VCAN, IGH-6, FN1, CXCL10	3.801185591
GO_CC	GO:0009897~external side of plasma membrane	4	0.01672055	LY6A, IGH-6, IGL-V1, FCGR1	7.14106225
GO_CC	GO:0031225~anchored to membrane	4	0.0169363	LY6A, LYNX1, LY6I, DPEP2	7.106564365
GO_CC	GO:0042571~immunoglobulin complex, circulating	2	0.01833283	IGHG, IGH-6	105.0756303
GO_CC	GO:0019815~B cell receptor complex	2	0.01833283	IGH-6, IGL-V1	105.0756303
GO_CC	GO:0043235~receptor complex	3	0.02011931	ITGA8, IGH-6, IGL-V1	13.29270021
GO_CC	GO:0005615~extracellular space	5	0.04420908	IGHG, CXCL2, CXCL9, IGH-6, CXCL10	3.598480488
GO_CC	GO:0009986~cell surface	4	0.04575733	LY6A, IGH-6, IGL-V1, FCGR1	4.823143684
GO_MF	GO:0001730~2'-5'-oligoadenylate synthetase activity	4	2.21E-06	OASL2, OAS1B, OAS1A, OAS2	134.2222222
GO_MF	GO:0016779~nucleotidyltransferase activity	7	3.53E-05	OASL2, OASL1, OAS1B, OAS3, OAS1A, OAS2, OAS1G	11.09711286
GO_MF	GO:0003823~antigen binding	6	4.34E-05	IGHG, IGK-V28, IGL-V2, IGH-6, IGL-V1, IGHV1-72	15.1
GO_MF	GO:0070566~adenylyltransferase activity	4	1.20E-04	OASL2, OAS1B, OAS1A, OAS2	40.26666667
GO_MF	GO:0003924~GTPase activity	6	3.99E-04	GBP6, IIGP1, TGTP1, MX1, MPA2L, MX2	9.4375
GO_MF	GO:0004869~cysteine-type endopeptidase inhibitor activity	4	9.00E-04	STFA2L1, STFA1, STFA3, STFA2	20.64957265
GO_MF	GO:0003723~RNA binding	11	0.00147216	IFIH1, OASL2, OASL1, OAS1B, OAS3, OAS1A, OAS2, EIF2AK2, OAS1G, DHX58, ZBP1	3.295634921
GO_MF	GO:0032553~ribonucleotide binding	19	0.00190168	GBP6, IFIH1, IRGM1, OAS3, SLFN8, SLFN5, OAS2, OASL2, OASL1, OAS1B, IIGP1, TGTP1, OAS1A, EIF2AK2, MX1, MPA2L, OAS1G, MX2, DHX58	2.129918337

GO_MF	GO:0032555~purine ribonucleotide binding	19	0.00190168	GBP6, IFIH1, IRGM1, OAS3, SLFN8, SLFN5, OAS2, OASL2, OASL1, OAS1B, IIGP1, TGTP1, OAS1A, EIF2AK2, MX1, MPA2L, OAS1G, MX2, DHX58	2.129918337
GO_MF	GO:0017076~purine nucleotide binding	19	0.00300946	GBP6, IFIH1, IRGM1, OAS3, SLFN8, SLFN5, OAS2, OASL2, OASL1, OAS1B, IIGP1, TGTP1, OAS1A, EIF2AK2, MX1, MPA2L, OAS1G, MX2, DHX58	2.044539462
GO_MF	GO:0005525~GTP binding	7	0.00755133	GBP6, IRGM1, IIGP1, TGTP1, MX1, MPA2L, MX2	3.981167608
GO_MF	GO:0032561~guanyl ribonucleotide binding	7	0.00849465	GBP6, IRGM1, IIGP1, TGTP1, MX1, MPA2L, MX2	3.882460973
GO_MF	GO:0019001~guanyl nucleotide binding	7	0.00849465	GBP6, IRGM1, IIGP1, TGTP1, MX1, MPA2L, MX2	3.882460973
GO_MF	GO:0003725~double-stranded RNA binding	3	0.01195093	OAS1B, OAS1A, EIF2AK2	17.76470588
GO_MF	GO:0008009~chemokine activity	3	0.01478965	CXCL2, CXCL9, CXCL10	15.89473684
GO_MF	GO:0000166~nucleotide binding	19	0.01502774	GBP6, IFIH1, IRGM1, OAS3, SLFN8, SLFN5, OAS2, OASL2, OASL1, OAS1B, IIGP1, TGTP1, OAS1A, EIF2AK2, MX1, MPA2L, OAS1G, MX2, DHX58	1.7523286
GO_MF	GO:0042379~chemokine receptor binding	3	0.01554042	CXCL2, CXCL9, CXCL10	15.48717949
GO_MF	GO:0004866~endopeptidase inhibitor activity	4	0.04418589	STFA2L1, STFA1, STFA3, STFA2	5.002070393
KEGG_PATHWAY	mmu04622:RIG-I-like receptor signaling pathway	5	1.35E-04	IFIH1, ISG15, IRF7, DHX58, CXCL10	17.57965686
KEGG_PATHWAY	mmu04062:Chemokine signaling pathway	5	0.00540468	CCR3, CXCL2, CXCL9, STAT1, CXCL10	6.568223443
KEGG_PATHWAY	mmu04620:Toll-like receptor signaling pathway	4	0.00686787	IRF7, CXCL9, STAT1, CXCL10	9.65993266
KEGG_PATHWAY	mmu04623:Cytosolic DNA-sensing pathway	3	0.02006538	IRF7, ZBP1, CXCL10	13.04090909